

Article

Synthesis of C₃-Symmetric Cinchona-Based Organocatalysts and Their Applications in Asymmetric Michael and Friedel–Crafts Reactions

Péter Kisszékelyi ^{1,*}, Zsuzsanna Fehér ¹, Sándor Nagy ¹, Péter Bagi ¹, Petra Kozma ¹, Zsófia Garádi ^{2,3}, Miklós Dékány ⁴, Péter Huszthy ¹, Béla Mátravölgyi ¹ and József Kupai ^{1,*}

¹ Department of Organic Chemistry & Technology, Budapest University of Technology & Economics, Szent Gellért tér 4, H-1111 Budapest, Hungary; zsuzsanna.feher@edu.bme.hu (Z.F.); nagy.sandor@mail.bme.hu (S.N.); bagi.peter@vbk.bme.hu (P.B.); pkozma@mail.bme.hu (P.K.); huszthy.peter@vbk.bme.hu (P.H.); matravolgyi.bela@vbk.bme.hu (B.M.)

² Department of Inorganic & Analytical Chemistry, Budapest University of Technology & Economics, Szent Gellért tér 4, H-1111 Budapest, Hungary; garadi.zsofia@pharma.semmelweis-univ.hu

³ Department of Pharmacognosy, Semmelweis University, Üllői út 26, H-1085 Budapest, Hungary

⁴ Spectroscopic Research Department, Gedeon Richter Plc., Gyömrői út 19-21, H-1103 Budapest, Hungary; M.Dekany@richter.hu

* Correspondence: kisszekelyi.peter@vbk.bme.hu (P.K.); kupai.jozsef@vbk.bme.hu (J.K.); Tel.: +36-1-463-2229 (J.K.)



Citation: Kisszékelyi, P.; Fehér, Z.; Nagy, S.; Bagi, P.; Kozma, P.; Garádi, Z.; Dékány, M.; Huszthy, P.; Mátravölgyi, B.; Kupai, J. Synthesis of C₃-Symmetric Cinchona-Based Organocatalysts and Their Applications in Asymmetric Michael and Friedel–Crafts Reactions. *Symmetry* **2021**, *13*, 521. <https://doi.org/10.3390/sym13030521>

Academic Editor: Yannick Vallée

Received: 28 February 2021

Accepted: 18 March 2021

Published: 23 March 2021

Publisher's Note: MDPI stays neutral with regard to jurisdictional claims in published maps and institutional affiliations.



Copyright: © 2021 by the authors. Licensee MDPI, Basel, Switzerland. This article is an open access article distributed under the terms and conditions of the Creative Commons Attribution (CC BY) license (<https://creativecommons.org/licenses/by/4.0/>).

Abstract: In this work, anchoring of cinchona derivatives to trifunctional cores (hub approach) was demonstrated to obtain size-enlarged organocatalysts. By modifying the cinchona skeleton in different positions, we prepared four C₃-symmetric size-enlarged cinchona derivatives (hub-cinchonas), which were tested as organocatalysts and their catalytic activities were compared with the parent cinchona (hydroquinine) catalyst. We showed that in the hydroxyalkylation reaction of indole, hydroquinine provides good enantioselectivities (up to 73% ee), while the four new size-enlarged derivatives resulted in significantly lower values (up to 29% ee) in this reaction. Anchoring cinchonas to trifunctional cores was found to facilitate nanofiltration-supported catalyst recovery using the PolarClean alternative solvent. The C₃-symmetric size-enlarged organocatalysts were completely rejected by all the applied membranes, whereas the separation of hydroquinine was found to be insufficient when using organic solvent nanofiltration. Furthermore, the asymmetric catalysis was successfully demonstrated in the case of the Michael reaction of 1,3-diketones and *trans*- β -nitrostyrene using **Hub³-cinchona** (up to 96% ee) as a result of the positive effect of the C₃-symmetric structure using a bulkier substrate. This equates to an increased selectivity of the catalyst in comparison to hydroquinine in the latter Michael reaction.

Keywords: cinchona; organocatalysis; C₃-symmetry; size-enlargement; nanofiltration; asymmetric reaction

1. Introduction

Over the years, catalysis has been widely explored for the more economical and often more selective production of high-value products [1]. As the preparation of enantiopure organic compounds is of great interest, asymmetric catalysis has developed into a dynamic, rapidly evolving field [2]. Compounds with rotational symmetry have gained increased attention in asymmetric synthesis because they are believed to be able to improve enantioselectivity by decreasing the number of possible transition states during the reaction [3–5]. Due to their beneficial effect on enantioselectivity, C₂- and C₃-symmetric molecules have been the focus of extensive research and, as a result, C₃-symmetric compounds have been successfully applied as catalysts, ligands, molecular receptors, supra- and macromolecular constructs, gelators, metal-organic materials (MOMs), etc. [6–11].

Organocatalysts containing three equal catalytic units in a C_3 -symmetrical fashion have also been studied. Following the application of tripodal phosphinamide ligands in the enantioselective BH_3 reduction of ketones [12,13], Han et al. successfully applied tribenzyl- and triphenylphosphine oxide-based proline organocatalysts for aldol reactions [14]. Subsequently, Moorthy et al. applied C_3 -symmetrical organocatalysts by anchoring proline and pyrrolidine to trifunctional trialkylbenzene cores. These C_3 -symmetric organocatalysts provided the Michael adducts of carbonyl compounds and *trans*- β -nitrostyrene with high stereoselectivities [15]. In addition to proline and pyrrolidine, *trisimidazoline* derivatives were also successfully utilized as catalysts by Fujioka et al. in Michael addition reactions, α -amination of β -ketoesters, and bromolactonization of alkenoic acids [16–18]. Later, the application of C_3 -symmetric *trisimidazoline* organocatalysts was extended to an enantio- and diastereoselective Betti/aza-Michael sequence as well [19].

Cinchona-based C_2 - and C_3 -symmetric compounds have also been widely studied [20]. Jew et al. demonstrated the high enantioselectivity of a novel trimeric cinchona alkaloid ammonium salt as a phase-transfer catalyst (PTC) in the catalytic asymmetric alkylation of the *N*-(diphenylmethylene)glycine *tert*-butyl ester [21]. Later, the C_3 -symmetric cinchona PTC catalyzed asymmetric synthesis of α -amino acids and the highly enantioselective Michael reaction of chalcones and diethyl malonate were performed by Siva et al. [22–25]. Csámpai and co-workers examined the *in vitro* antitumor activity of acylated *mono*-, *bis*-, and *tris*-cinchona-based amines [26]. Other than high selectivity, Dong et al. also showed the good recyclability of cinchonine squaramide-based C_3 -symmetric catalysts in enantioselective Michael addition, in hydroxyalkylation of indoles with alkyl trifluoropyruvate, and in asymmetric chlorolactonization of carboxylic acids [27–30]. These catalysts were easily recovered by precipitation and used for four to six cycles without significant loss of productivity or selectivity.

Organic solvent nanofiltration (OSN), also called solvent-resistant nanofiltration (SRNF), is a pressure-driven sustainable separation technology applied in fine chemical and petrochemical purification, which can separate solutes between 50 and 2000 $g\ mol^{-1}$ in a wide range of organic solvents [31]. OSN is a predictable and energy-efficient technology compared to other separation techniques such as distillation, chromatography, and extraction [32]. There is increasing interest in applying OSN for the purification of pharmaceutically relevant compounds [33–36], as well as for solvent recovery [37,38]. OSN has also been proposed for the recovery of enlarged metal catalysts [39], and organocatalysts [40]. As an alternative recycling method to precipitation, Livingston et al. demonstrated the OSN enabled recovery of C_3 -symmetric quinidine-based organocatalysts [41]. The immobilization of cinchonins on trifunctional cores was found to be an effective molecular weight enlargement (MWE) method to facilitate their retention by OSN without destroying the catalytic efficiency of the organocatalysts in Michael addition reactions. Immobilizing organocatalysts on multifunctional cores, the so-called “hub-approach”, is an MWE method, in which the number of catalytic motifs in the size-enlarged molecule is increased, while the extent of non-functional “spacers” is decreased in comparison to polymer- or dendrimer-based supports. By adjusting the length and type of the linkers between the core (hub) and the catalytic units, the rigidity of the resulting size-enlarged catalyst can be regulated, which has a direct effect on the selectivity experienced in the organocatalytic reactions.

Taking these results into account, we intended to further explore the organocatalytic opportunities of size-enlarged C_3 -symmetric cinchona-based organocatalysts. Thus, multiple hub-cinchona structures both with or without H-bond donor capabilities were designed and tested in the hydroxyalkylation of indole and Michael addition reactions, in which the structure–selectivity relationships are also discussed. Finally, the expected superior membrane rejection of the size-enlarged catalysts is presented.

2. Results

During our work, we prepared and explored two types of C_3 -symmetric cinchona organocatalysts with varied H-bond donor properties (Figure 1). Compounds belonging

to Type A are structurally the simplest as they have no H-bond donor units due to the derivatization of the hydroxyl group (9-OH, see Figure 1c) of the cinchona skeleton during the immobilization process. On the contrary, the mono H-bond donor 9-OH has been reserved in the case of Type B compounds as the cinchona motif was anchored to the hub, either through the aromatic quinoline (Williamson ether formation) or through the quinuclidine unit using copper(I) catalyzed azide–alkyne cycloaddition (CuAAC). As a hub, we used 1,3,5-triethynylbenzene, 1,3,5-tris(bromomethyl)benzene, or tripropargylamine.

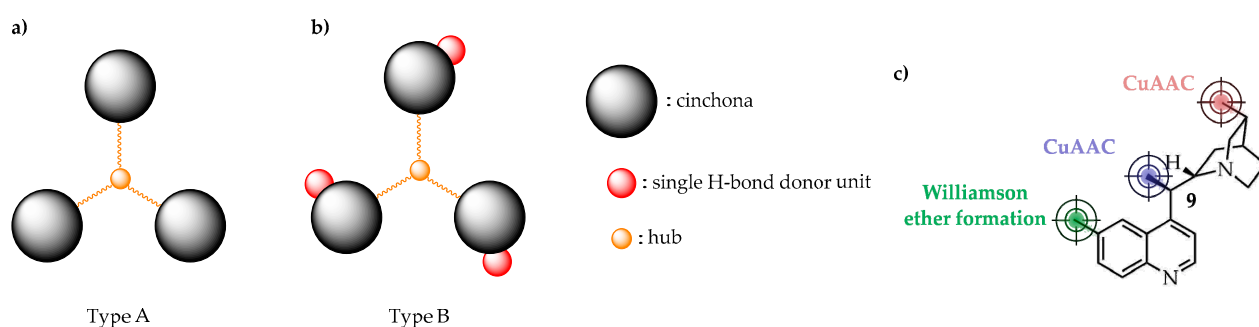


Figure 1. We explored C_3 -symmetric hub-cinchona structures containing no (a), or single H-bond donor units (b). Cinchona skeleton was anchored through different positions (c). CuAAC: copper(I) catalyzed azide–alkyne cycloaddition.

2.1. Synthesis of New C_3 -Symmetric Hub-Cinchona Catalysts

First, we prepared **Hub^{1,2}-cinchona** (Type A) organocatalysts using a common intermediate (**3**, Scheme 1). Cinchona azide **3** was obtained in two steps: mesylation of hydroquinine (**1**), followed by substitution with azide anion applying NaN_3 . Then, azide **3** was reacted with either 1,3,5-triethynylbenzene (**4**), or tripropargylamine (**5**) in a CuAAC reaction, which gave **Hub¹-** and **Hub²-cinchona**, respectively, with moderate yields. Having been functionalized at the secondary hydroxyl group of the cinchona moiety, these compounds contain no H-bond donor units. However, other non-covalent interactions can still be formed through the protonated quinuclidine N-atom (ionic) or the aromatic quinoline ring (π – π stacking). Furthermore, the triazole-rings formed by the CuAAC reaction are good electron pair donors, which could interact with metallic species, combining the advantageous catalytic qualities of organocatalysts and transition metals to promote new chemical transformations [42,43].

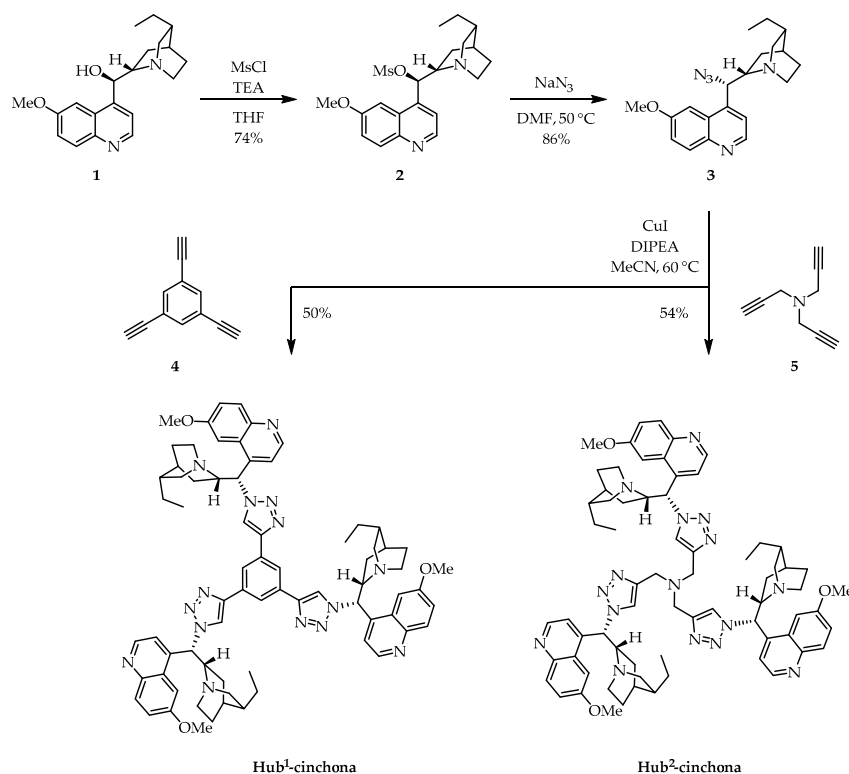
Next, cinchona derivatives with mono H-bond donor units (Type B) have been prepared. Hydroquinine (**1**) was demethylated using BBr_3 (1M in DCM) to obtain dihydrocupreine **6** that bears a free phenolic hydroxyl group (Scheme 2). Then, using Cs_2CO_3 as a base, the phenolate of **6** was formed, which could react with 1,3,5-tris(bromomethyl)benzene (**7**) in a Williamson ether formation reaction to give the size-enlarged organocatalyst **Hub³-cinchona** with a good yield. Consequently, we connected the cinchona motif to the core through a stable ether bond, and the H-bond donor hydroxyl group remained intact.

Organocatalyst **Hub⁴-cinchona** was prepared via convergent synthesis (Scheme 3), utilizing an alternative anchoring method. We converted the commercially available quinine (**8**) into didehydroquinine (**9**) using a Br_2 addition–HBr elimination reaction. In a separate reaction, we reacted 1,3,5-tris(bromomethyl)benzene (**7**) with NaN_3 in a mixture of water:acetone (1/100) to give the triazido-derivative **10**. Finally, alkyne **9** and triazide **10** were subjected to a CuAAC reaction, which gave organocatalyst **Hub⁴-cinchona** with a moderate yield.

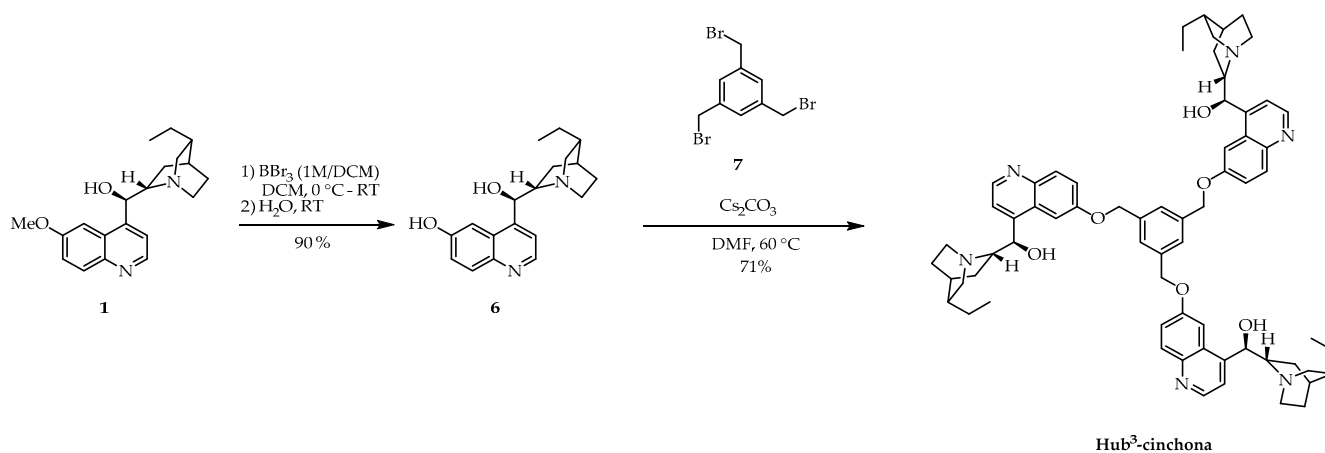
2.2. Application of Hub-Cinchona Catalysts in Hydroxyalkylation of Indole and Michael Addition Reactions

We started our organocatalytic reactions with the hydroxyalkylation of indole. First, the optimal solvent and reaction time were chosen using 5 mol% hydroquinine (**1**), the parent catalytic unit of the hub-cinchona derivatives. As solvents, 11 conventional and

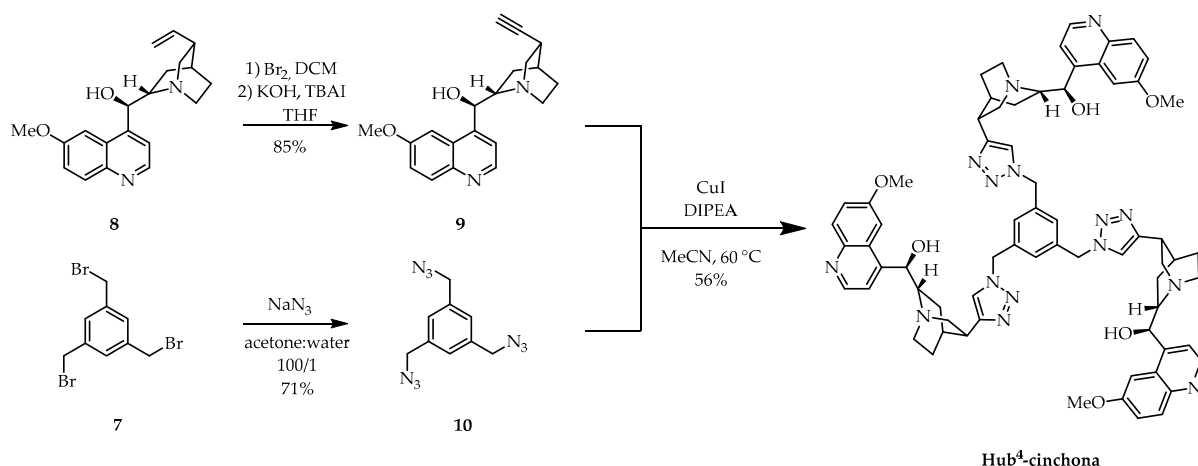
alternative agents were used (Table 1). In general, ether-type solvents showed better enantioselectivities in this reaction, while the protic ethanol gave a practically racemic product. An explanation for this solvent effect could be the formation of competing H-bonds between the solvent and the catalyst/substrates. Regarding the yield, in toluene and ethanol we achieved almost complete transformation, while the other solvents also gave good results (>67%). For the subsequent experiments, cyclopentyl methyl ether (CPME) was chosen, because this solvent provided the best enantioselectivity (73% ee) and the yield was still good after 24 h stirring at 0 °C (82%). Based on the ^{19}F NMR spectra, the yield did not change significantly when the reaction time was reduced to 1 h.



Scheme 1. Syntheses of the size-enlarged C_3 -symmetric **Hub¹-** and **Hub²-cinchona** organocatalysts (Type A) by CuAAC using a common cinchona azide intermediate (**3**) and trifunctional alkynes (**4** or **5**) with different chemical and structural properties. TEA: triethylamine; MsCl: methanesulfonyl chloride; DIPEA: *N,N*-diisopropylethylamine.



Scheme 2. Synthesis of the size-enlarged C_3 -symmetric **Hub³-cinchona** organocatalyst by Williamson ether formation.



Scheme 3. Convergent synthesis of size-enlarged C₃-symmetric **Hub⁴-cinchona** organocatalyst by CuAAC using a triazide core unit (**10**). TBAI: tetra-*n*-butylammonium iodide; DIPEA: *N,N*-diisopropylethylamine.

Table 1. Hydroquinine (**1**) catalyzed indole hydroxyalkylation reaction in different solvents ¹.

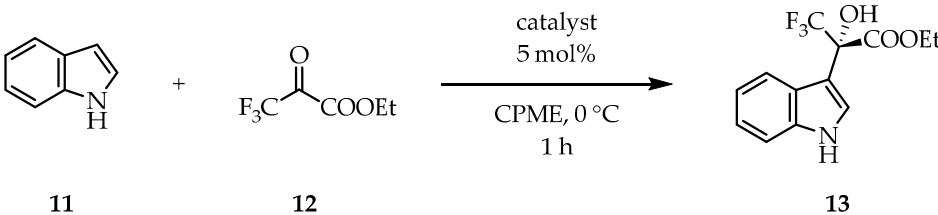
Solvent	Reaction Time (h)	Yield (13 , %) ²	Enantiomeric Excess [(<i>S</i>), %] ³
CPME	24	82	73
2-MeTHF	24	70	69
MTBE	24	88	67
DME	24	81	64
toluene	24	98	61
EtOAc	24	70	59
PolarClean	24	67	52
DMC	24	92	52
DCM	24	99	48
MeCN	24	82	36
EtOH	24	98	2
CPME	4	87	73
CPME	2	85	72
CPME	1	87	72

¹ Reaction conditions: indole (1 eq), ethyl trifluoropyruvate (1 eq), 0.015 mmol catalyst mL⁻¹ solvent; ² Determined by ¹⁹F NMR; ³ Determined by chiral HPLC; CPME: cyclopentyl methyl ether; 2-MeTHF: 2-methyltetrahydrofuran; MTBE: *tert*-butyl methyl ether; DME: dimethoxyethane; PolarClean: methyl 5-(dimethylamino)-2-methyl-5-oxopentanoate; DCM: dichloromethane.

With the best solvent and reaction time in hand, we used our newly prepared hub-cinchona organocatalysts in the hydroxyalkylation reaction (Table 2). While the yield was only slightly lower (~10% difference), the size-enlarged catalysts showed significantly lower enantioselectivities in comparison to hydroquinine (**1**). The highest enantiomeric excess was achieved with **Hub⁴-cinchona** (29% ee), while **Hub²-cinchona** practically provided the hydroxyalkylated product as a racemic mixture (2% ee). Due to the tripropargylamine hub, the latter catalyst (**Hub²-cinchona**) contains a competitive basic unit with the quinuclidine N-atom, which can explain the lack of enantioselectivity. Comparing the structural features of the other catalysts, we can conclude that **Hub¹-** and **Hub⁴-cinchonas** have more rigid structures, which can be attributed to the triazole rings that also serve as spacers between

the hub and the catalytically active motifs. Therefore, the cinchona units in these cases are more separated from each other. Still, the formation of non-covalent interactions between the individual catalytic motifs within the hub-cinchonas can explain, in general, the significantly lower enantioselectivity and why **Hub^{1,4}-cinchonas** gave better results than the structurally more flexible **Hub³-cinchona**. The Structures, NMR spectra, MS spectra and HPLC chromatograms of the prepared C₃-symmetric hub-cinchonas (Hub1-4-cinchonas) are shown in Supplementary Materials.

Table 2. Hydroquinine (**1**) and **Hub¹⁻⁴-cinchonas** catalyzed indole hydroxyalkylation reaction ¹.

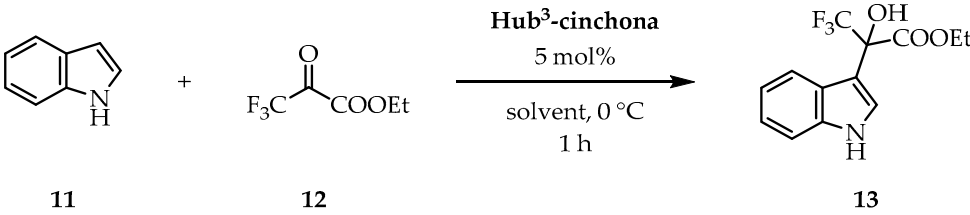


Catalyst	Yield (13 , %) ²	Enantiomeric Excess [(S), %] ³
hydroquinine (1)	87	72
Hub¹-cinchona	78	26
Hub²-cinchona	77	2
Hub³-cinchona	69	18
Hub⁴-cinchona	72	29

¹ Reaction conditions: indole (1 eq), ethyl trifluoropyruvate (1 eq), 0.016 mmol catalyst mL⁻¹ solvent; ² Determined by ¹⁹F NMR; ³ Determined by chiral HPLC.

As the solvent can significantly alter the formation of non-covalent interactions, we performed the complete solvent screen with **Hub³-cinchona** (Table 3). While no higher enantioselectivity was achieved, the previously observed trend was still recognizable: ether-type solvents gave good results, but the protic ethanol promoted the formation of the racemic product. Interestingly, in some cases (toluene, DCM, and MeCN) the other antipode of **13** was found to be present in excess.

Table 3. **Hub³-cinchona** catalyzed indole hydroxyalkylation reaction in different solvents ¹.



Solvent	Enantiomeric Excess (13 , %) ²	Solvent	Enantiomeric Excess (13 , %) ²
CPME	18 (S)	PolarClean	10 (S)
2-MeTHF	12 (S)	DMC	4 (S)
MTBE	12 (S)	DCM	11 (R)
DME	13 (S)	MeCN	13 (R)
toluene	4 (R)	EtOH	0
EtOAc	2 (S)		

¹ Reaction conditions: indole (1 eq), ethyl trifluoropyruvate (1 eq), 0.0165 mmol catalyst mL⁻¹ solvent; ² Determined by chiral HPLC; CPME: cyclopentyl methyl ether; 2-MeTHF: 2-methyltetrahydrofuran; MTBE: *tert*-butyl methyl ether; DME: dimethoxyethane; PolarClean: methyl 5-(dimethylamino)-2-methyl-5-oxopentanoate; DCM: dichloromethane.

Additionally, the catalytic efficiencies of the size-enlarged hub-cinchonas and hydroquinine (**1**) were also compared in the Michael addition reaction of pentane-2,4-dione (**14**) and *trans*- β -nitrostyrene (**15**). The applied reaction conditions were chosen based

on our previous work [44]. Based on the measured enantioselectivities (Table 4), hydroquinine (**1**) is not a suitable catalyst for this reaction (14% ee). While organocatalysts **Hub**^{1,2,4}-cinchonas gave nearly racemic mixtures, **Hub**³-cinchona showed two times higher enantioselectivity than catalyst **1** (32% ee vs. 14% ee) with a preference to the mirror image stereoisomer.

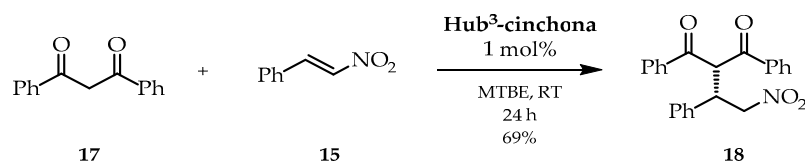
Table 4. Hydroquinine (**1**) and hub-cinchona catalyzed Michael addition reaction of pentane-2,4-dione (**14**) and *trans*- β -nitrostyrene (**15**)¹.

Catalyst	Yield (16 , %) ³	Enantiomeric Excess (16 , %) ²
hydroquinine (1)	82	14 (<i>R</i>)
Hub ¹ -cinchona	10	3 (<i>S</i>)
Hub ² -cinchona	24	1 (<i>S</i>)
Hub ³ -cinchona	82	32 (<i>S</i>)
Hub ⁴ -cinchona	78	1 (<i>S</i>)

¹ Reaction conditions: diketone (2.5 eq), nitrostyrene (1 eq), 0.015 mmol catalyst mL⁻¹ solvent; ² Determined by chiral HPLC; ³ Yield of isolated product purified by preparative thin-layer chromatography (TLC).

Considering that these two catalysts (**1** and **Hub**³-cinchona) are structurally very similar in regard to the catalytical motif(s), the higher selectivity clearly suggests that the C₃-symmetric structural feature of the size-enlarged **Hub**³-cinchona has a positive effect on the enantioselectivity. This advantageous outcome can be attributed either to the formation of a sterically more hindered space during the transition state or to an alternative catalyst–substrate interaction layout including two or more cinchona motifs.

Next, using **Hub**³-cinchona, the Michael addition reaction was also performed with a structurally bulkier and electronically more favorable Michael donor, 1,3-diphenylpropane-1,3-dione (**17**, Scheme 4). The applied reaction conditions were based on our previous work [45]. Although only 1 mol% of catalyst was used, the enantioselectivity observed was significantly higher regardless of the solvent (2 mL), e.g., DCM (53% ee), EtOAc (64% ee), MeCN (71% ee), or toluene (80% ee). The best result was achieved by using MTBE. In this case, the selectivity reached 93% ee and the yield was 69% after purification by preparative thin-layer chromatography (TLC). In comparison, the reaction catalyzed by hydroquinine (**1**) gave only 6% ee with an 84% preparative yield.



Scheme 4. Michael addition of 1,3-diphenylpropane-1,3-dione (**17**) and *trans*- β -nitrostyrene (**15**) catalyzed by **Hub**³-cinchona organocatalyst.

To conclude, the Michael addition reaction showed increased selectivity for the size-enlarged **Hub**³-cinchona catalysts compared to its cinchona unit (hydroquinine, **1**), which indicates the positive effect of the C₃-symmetric structure. Furthermore, a Michael adduct prepared from the bulkier substrate was obtained with excellent enantioselectivities (up to 93% ee) with **Hub**³-cinchona size-enlarged organocatalyst.

2.3. Membrane Rejection of Hub-Cinchona Organocatalysts

Given the bulky nature of the size-enlarged catalysts, they were fully retained on all the tested membranes with rejection values of 100% (Figure 2a). It is important to achieve 100%

rejection in order to avoid the loss of any valuable catalyst during the recovery process. The rejections of indole (**11**) and the hydroxyalkylated product **13** vary between 5% and 55% depending on both the membrane and the molecular weight (MW). For efficient catalyst recovery, the rejection gap between the catalyst and the other solutes needs to be as large as possible. Consequently, one can conclude that the best membrane for hub-cinchona organocatalyst recovery is DM900. This membrane exhibited substrate solute rejections below 30%, while still maintaining complete retention of the catalysts. Moreover, DM900 is the most open membrane with the highest flux of $6.7 \pm 0.24 \text{ L m}^{-2} \text{ h}^{-1}$ (Figure 2b). It is important to maximize the flux in order to achieve an efficient catalyst recovery process. Comparing the membrane rejections of the hub-cinchonas with hydroquinine (**1**), the advantage of molecular size-enlargement can be clearly seen. Due to the similar rejection values of hydroquinine (**1**) and product **13**, membrane recovery of **1** from the reaction mixture would be inadequate.

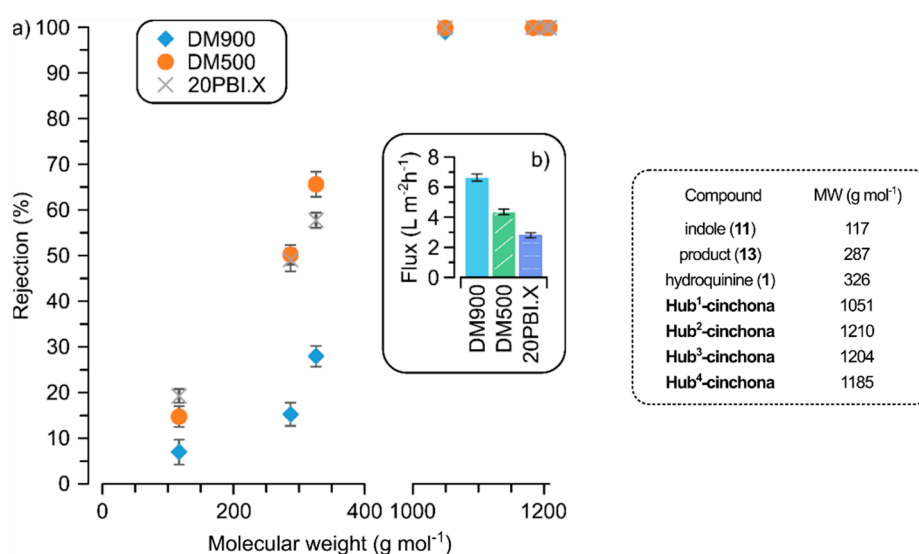


Figure 2. Rejection (a) and flux (b) values for the three screened solvent-resistant membranes in PolarClean green solvent at 10 bar in crossflow mode.

3. Materials and Methods

3.1. General Information

Starting materials were purchased from commercially available sources (Sigma-Aldrich, Merck, and Alfa Aesar). Infrared spectra were recorded on a Bruker Alpha-T FT-IR spectrometer (Bruker, Ettlingen, Germany). Optical rotations were measured on a Perkin-Elmer 241 polarimeter (Perkin-Elmer, Waltham, MA, USA) that was calibrated by measuring the optical rotations of both enantiomers of menthol. Silica gel 60 F₂₅₄ (Merck) and aluminum oxide 60 F₂₅₄ neutral type E (Merck) plates were used for TLC. Aluminum oxide (neutral, activated, Brockman I) and silica gel 60 (70–230 mesh, Merck) were used for column chromatography. Ratios of solvents for the eluents are given in volumes (mL mL⁻¹). Melting points were taken on a Boetius micro-melting point apparatus (VEB Dresden Analytik, Dresden, Germany) and they were uncorrected. *N,N*-Dimethylacetamide (DMAc) solution of polybenzimidazole (PBI, 26 wt%) was purchased from PBI Performance Products (USA). The previously reported 20PBI.X membrane was obtained based on Schaepertoens et al. [46]. PBI was selected as it is an emerging polymer for OSN [47,48]. DuraMem solvent-resistant membranes (DM500 and DM900) can be obtained from Evonik (Germany). PolarClean solvent is produced by Solvay (Italy). NMR spectra were recorded either on a Bruker DRX-500 Avance spectrometer (at 500 MHz for ¹H, at 125 MHz for ¹³C, and at 376 MHz for ¹⁹F spectra) or on a Bruker 300 Avance spectrometer (at 300 MHz for ¹H, at 75 MHz for ¹³C, and at 222.5 MHz for ¹⁹F spectra) or on a Bruker Avance III HD (at 600 MHz for ¹H and at 150 MHz for ¹³C spectra). HPLC-MS was performed on an HPLC

system using Agilent Technologies 1200 Series-Agilent Technologies 6130 Quadrupole; column: Phenomenex Kinetex C18 100A (2.6 μm , 50 \times 3.00 mm); A eluent: water (1% HCOONH_4); B eluent: MeCN (8% water, 1% HCOONH_4); gradient: 20–100%. In case of indole hydroxyalkylation, HPLC-MS was performed using a Shimadzu LCMS-2020 (Shimadzu Corp., Kyoto, Japan) device, equipped with a Reprospher (Altmann Analytik Corp., München, Germany) 100 C18 (5 μm , 100 \times 3 mm) column and a positive/negative double ion source (DUIS \pm) with a quadrupole MS analyzer in a range of 50–1000 m/z . The samples were eluted with gradient elution, using eluent A (0.1% formic acid in water) and eluent B (0.1% formic acid in MeCN). The flow rate was set to 1.5 mL min^{-1} . The initial condition was 5% eluent B, followed by a linear gradient to 100% eluent B by 1.5 min; from 1.5 to 4.0 min, 100% eluent B was retained, and from 4 to 4.5 min, it went back by a linear gradient to 5% eluent B, which was retained from 4.5 to 5 min. The column temperature was kept at room temperature, and the injection volume was 1–10 μL . The purity of the compounds was assessed by HPLC with UV detection at 215 and 254 nm. High resolution mass measurements were performed on a Thermo Exactive plus EMR Orbitrap mass spectrometer, which was used with a Thermo Ultimate 3000 UHPLC with 100% methanol as the mobile phase, or on a Thermo Velos Pro Orbitrap Elite (Thermo Fisher Scientific) system. The ionization method was ESI operated in positive ion mode. The samples were dissolved in methanol. Data acquisition and analysis were accomplished with Xcalibur software version 4.0 (Thermo Fisher Scientific). The enantiomeric ratios of the samples were determined by chiral high-performance liquid chromatography (HPLC) measurements using either reversed-phase mode (Thermo Finnigan Surveyor LC System, Thermo Fisher Scientific, Waltham, MA, USA) or normal phase mode (PerkinElmer Series 200 LC System, PerkinElmer, Inc, Shelton, CT, USA), and the exact conditions are indicated in the correspondent asymmetric reaction in the Experimental Section.

3.2. Preparation of Compounds

(1R)-(–)-((2S,4S,5R)-5-Ethylquinuclidin-2-yl)(6-methoxyquinolin-4-yl)methyl methanesulfonate (2):

This compound was prepared based on the description in the literature [49]. A solution of hydroquinine (**1**, 3.00 g, 9.19 mmol, 1.0 eq) in dry tetrahydrofuran (THF, 55 mL) was stirred under Ar at 0 °C. Triethylamine (TEA, 6.2 mL, 44.1 mmol, 4.8 eq) was added to this solution, followed by dropwise addition of methanesulfonyl chloride (2.9 mL, 36.8 mmol, 4.0 eq). Next, the reaction mixture was allowed to warm up to room temperature, and it was stirred for 4 h. The solvent was evaporated under reduced pressure. The residue was dissolved in a mixture of DCM (50 mL) and sat. aqueous solution of NaHCO_3 (50 mL). The aqueous phase was extracted with DCM (2 \times 50 mL). The combined organic phase was dried over anhydrous MgSO_4 , filtered, and the solvent was removed under reduced pressure. The crude product was purified by column chromatography (silica gel, MeOH/toluene 1:6) to obtain hydroquinine mesylate (**2**, 2.20 g, 73%) as a yellow solid.

R_f : 0.37 (silica gel, MeOH/toluene 1:4); Mp: 102.9–104.3 °C (lit Mp: 105–108 °C) [48]; MS-ESI+ (m/z): $[\text{M} + \text{H}]^+$ calculated for $\text{C}_{21}\text{H}_{29}\text{N}_2\text{O}_4\text{S}$: 405.2, found: 405.0. Spectroscopic data are fully consistent with those reported in the literature [50].

(2S,4S,5R)-(+)-2-((S)-Azido(6-methoxyquinolin-4-yl)methyl)-5-ethylquinuclidine (3):

Compound **3** was prepared based on the description in the literature [49]. A solution of mesylate **2** (2.00 g, 4.94 mmol, 1.0 eq) in dry dimethylformamide (DMF, 55 mL) was stirred under Ar atmosphere at room temperature. NaN_3 was then added (1.45 g, 22.3 mmol, 4.5 eq) to this solution. Next, the reaction mixture was warmed up to 45 °C and it was stirred at this temperature until the reaction was completed. The solvent was evaporated under reduced pressure, then, water was added to the residue, and this aqueous mixture was extracted with Et_2O (3 \times 15 mL). The combined organic phase was evaporated to obtain azido-hydroquinine as a yellow oil (**3**, 1.44 g, 83%) and used without further purification.

R_f: 0.20 (silica gel, DCM/MeOH 10:1); MS-ESI+ (*m/z*): [M + H]⁺ calculated for C₂₀H₂₆N₅O₄: 352.2, found: 352.1. Spectroscopic data are fully consistent with those reported in the literature [44,51].

Dihydrocupreine (6):

Hydroquinine (**1**, 1.00 g, 3.06 mmol, 1.0 eq) was dissolved in DCM (90 mL) under an Ar atmosphere, then this solution was cooled to 0 °C. Next, BBr₃ (1 M DCM solution, 26.0 mL, 26.0 mmol, 8.5 eq) was added dropwise. Next, the reaction mixture was left to slowly warm up to room temperature, and it was stirred overnight. After complete consumption of the starting material (TLC, silica gel, DCM/MeOH/NH₄OH 5:1:0.01), a solution of 10% NaOH (aq., 40 mL) was added to the mixture. Following the separation of the two phases, the aqueous phase was washed with DCM (3 × 50 mL). Next, cc. HCl (aq.) was added to neutralize the aqueous phase, followed by extraction with DCM (3 × 50 mL). The combined organic phase was dried over anhydrous MgSO₄, filtered, and the solvent was evaporated under reduced pressure to yield **6** (860 mg, 90%) as a brown solid.

R_f: 0.12 (silica gel; MeOH/toluene 1:4); [α]_D²⁵: -180.9° (c 1.00, CHCl₃); Mp. 224.4–225.9 °C (lit. Mp. 230 °C, [52]). Spectroscopic data are fully consistent with those reported in the literature [53].

(R)-[(2S,4S,5S)-5-Ethynylquinuclidine-2-yl](6-methoxyquinoline-4-yl)methanol (9)

To a solution of quinine (**8**, 5.00 g, 15.4 mmol, 1.0 eq) in DCM (150 mL), a mixture of Br₂ (1.70 mL, 30.9 mmol, 2.0 eq) and DCM (7 mL) was added at 0 °C. The reaction mixture was stirred at 0 °C for 1 h while a yellow solid precipitated. After stirring the reaction mixture for an additional hour at room temperature, hexane (300 mL) was added, stirred for 10 min, and filtered. The filtrate was washed with hexane and dried under infrared lamp for 1 h. The yellow solid was dissolved in THF (150 mL), and tetrabutylammonium iodide (TBAI, 550 mg, 1.71 mmol, 0.1 eq) was added to this solution. Then, finely powdered potassium hydroxide (KOH, 5.00 g, 89.1 mmol, 5.8 eq) was added to the mixture, and stirred at 45 °C for 1 h when an additional batch of KOH (5.00 g, 89.1 mmol, 5.8 eq) was added to it. The reaction mixture was stirred for 12 h at room temperature. After complete consumption of the starting materials (TLC, silica gel, MeOH/DCM/TEA 1:10:0.2), the mixture was filtered, dried over anhydrous MgSO₄, and the solvent was removed under reduced pressure. The crude product was purified by dry column vacuum chromatography (silica gel, EtOAc/NH₄OH 20:1, EtOAc/NH₄OH/MeOH 95:5–45:55) to yield **9** (4.25 g, 85%) as a brown solid.

R_f: 0.50 (silica gel, MeOH/DCM/TEA 1:10:0.2). Mp. 167–170 °C; Spectroscopic data are fully consistent with those reported in the literature [54].

1,3,5-Tris(azidomethyl)benzene (10)

Tris(bromomethyl)benzene (**7**, 500 mg, 1.40 mmol, 1.0 eq) was dissolved in a mixture of acetone/H₂O 1:0.01 (10 mL), then NaN₃ (550 mg, 8.50 mmol, 6.1 eq) was added, and the resulting mixture was stirred at room temperature for 1 day. After consumption of the starting material (TLC, silica gel, EtOAc/hexane 1:2), the mixture was concentrated, and to the remaining aqueous mixture EtOAc (15 mL) and water (15 mL) were added. The separated organic phase was washed with water (2 × 15 mL), dried over anhydrous MgSO₄, filtered, and the solvent was removed under reduced pressure to yield **10** (244 mg, 71%) as an oil. This product was used without further purification.

R_f: 0.65 (silica gel, EtOAc/hexane 1:2). Spectroscopic data are fully consistent with those reported in the literature [54]. Although the tris(azidomethyl)benzene is reported to be relatively insensitive to heat and shock, special care was taken during its synthesis and application to avoid accidents [55,56].

Hub¹-cinchona

To a mixture of cinchona azide (**3**, 700 mg, 2.00 mmol, 6.0 eq), 1,3,5-triethynylbenzene (**4**, 50 mg, 0.33 mmol, 1.0 eq) and *N,N*-diisopropylethylamine (DIPEA, 1.22 mL, 7.00 mmol, 21.0 eq) a suspension of CuI (38 mg, 0.20 mmol, 0.6 eq) in MeCN (1 mL) was added.

The mixture was stirred at 60 °C for 2 days. After complete consumption of the starting material (TLC, silica gel, MeOH/DCM/NH₄OH 1:10:0.01), the solvent was evaporated under reduced pressure, and the crude product was purified by column chromatography (silica gel, MeOH/DCM/NH₄OH 1:20:0.01–1:5:0.01 to yield **Hub¹-cinchona** (200 mg, 50%) as light-yellow solid.

R_f: 0.40 (silica gel, MeOH/DCM/NH₄OH 1:10:0.01); Mp. 195 °C; ¹H NMR (600 MHz, DMSO-d₆): δ 0.85 (m, 12H), 1.40 (m, 12H), 1.53 (overlapping, 3H), 1.63 (br, 6H), 1.73 (br, 3H), 2.41 (m, 3H), 2.96 (m, 3H), 3.43 (overlapping, 3H), 3.99 (s, 9H), 4.09 (overlapping, 3H), 6.64 (m, 3H), 7.46 (m, 3H), 7.85 (br, 3H), 7.88 (d, *J* = 6.0 Hz, 3H), 7.98 (d, *J* = 6.0 Hz, 3H), 8.11 (m, 3H), 8.86 (m, 6H); ¹³C NMR (125 MHz, DMSO-d₆): δ 12.3, 25.4, 26.5, 27.3, 28.0, 37.0, 40.7, 56.0, 57.0, 57.1, 59.7, 102.5, 120.6, 121.1, 121.2, 121.7, 127.9, 131.7, 132.1, 140.0, 144.4, 145.6, 148.1, 158.0; HPLC-MS-ESI⁺ (*m/z*): [M + H]⁺ calculated for C₇₂H₈₂N₁₅O₃: 1204.66, found: 1204.44; triflate salt formed by the addition of Cu(CF₃SO₃)₂: HRMS-ESI⁺ (*m/z*): [(M + 2H + Tf)/2]²⁺ calculated for C₇₃H₈₄O₆N₁₅F₃S: 677.81954; found: 677.81628.

Hub²-cinchona

To a mixture of cinchona azide (**3**, 803 mg, 2.29 mmol, 6.0 eq), tripropargylamine (**5**, 50 mg, 0.38 mmol, 1.0 eq) and DIPEA (1.39 mL, 8.00 mmol, 21.0 eq) was added a suspension of CuI (44 mg, 0.23 mmol, 0.6 eq) in MeCN (1 mL). The mixture was stirred at 60 °C for 2 days. After complete consumption of the starting material (TLC, silica gel, MeOH/DCM/NH₄OH 1:10:0.01), the solvent was evaporated under reduced pressure, and the crude product was purified by column chromatography (silica gel, MeOH/DCM/NH₄OH 1:20:0.01–1:5:0.01 to yield **Hub²-cinchona** (243 mg, 54%) as light-yellow solid.

R_f: 0.40 (silica gel, MeOH/DCM/NH₄OH 1:10:0.01); Mp. 162 °C; ¹H NMR (600 MHz, DMSO-d₆): δ 0.73 (br, 3H), 0.82 (m, 9H), 1.35 (overlapping, 12H), 1.60 (overlapping, 9H), 2.33 (br, 3H), 2.46 (br, 3H), 2.90 (br, 3H), 3.42 (overlapping, 9H), 3.89 (s, 9H), 3.98 (br, 3H), 6.52 (br, 3H), 7.43 (m, 3H), 7.74 (br, 3H), 7.82 (m, 3H), 7.96 (d, *J* = 9.0 Hz, 3H), 8.16 (overlapping, 3H), 8.78 (m, 3H); ¹³C NMR (125 MHz, DMSO-d₆): δ 12.3, 25.3, 26.4, 27.1, 28.1, 37.0, 40.7, 46.8, 56.0, 57.0, 57.4, 59.3, 102.3, 120.8, 121.7, 123.9, 127.9, 131.7, 140.3, 142.5, 144.4, 147.9, 158.0; HPLC-MS-ESI⁺ (*m/z*): [M + H]⁺ calculated for C₆₉H₈₅N₁₆O₃: 1185.69, measured: 1185.55; HRMS-ESI⁺ (*m/z*): [M + H]⁺ calculated for C₆₉H₈₅N₁₆O₃: 1185.6985, found: 1185.6951.

Hub³-cinchona

To a solution of dihydrocupreine (**6**, 500 mg, 1.60 mmol, 6.0 eq) in dry DMF (50 mL), Cs₂CO₃ (772 mg, 2.39 mmol, 9.0 eq) was added, and the resulting mixture was stirred at 60 °C for 1 h. Next, 1,3,5-*tris*(bromomethyl)benzene (**7**, 95 mg, 0.27 mmol, 1.0 eq) was added to the mixture, and stirred for 3 h. Then, the solvent was evaporated, and the residue was taken up in a mixture of EtOAc (50 mL) and H₂O (50 mL). The forming brown precipitate was filtered and washed with EtOAc (3 × 20 mL) to yield **Hub³-cinchona** (398 mg, 71%) as a brown solid.

R_f: 0.41 (aluminum oxide, MeOH/DCM/NH₄OH 10:1:0.01); Mp. 166–175 °C; IR (film) ν_{max}: 3267, 2929, 2871, 1618, 1590, 1507, 1457, 1378, 1359, 1325, 1238, 1217, 1131, 1115, 1085, 1052, 1024, 1004, 937, 880, 857, 820, 758, 693, 642, 620, 609, 568, 549, 530, 467, 435, 417, 401 cm⁻¹; ¹H NMR (600 MHz, DMSO-d₆): δ: 0.76 (t, *J* = 7 Hz, 9H), 1.22 (m, 6H), 1.25 (m, 3H), 1.28 (m, 3H), 1.57 (m, 3H), 1.61 (m, 3H), 1.64 (m, 3H), 1.65 (m, 3H), 2.06 (m, 3H), 2.31 (m, 3H), 2.75 (m, 3H), 2.98 (m, 3H), 3.10 (br, 3H), 5.20 (br, 3H), 5.32 (d, *J* = 12.6 Hz, 3H), 5.34 (d, *J* = 12.6 Hz, 3H), 5.67 (br, 3H), 7.47 (dd, *J* = 9.1 Hz, 2.7 Hz, 3H), 7.50 (d, *J* = 4.5 Hz, 3H), 7.64 (br d, *J* = 2.7 Hz, 3H), 7.66 (br, 3H), 7.94 (d, *J* = 9.1 Hz, 3H), 8.68 (d, *J* = 4.5 Hz, 3H); ¹³C NMR (125 MHz, DMSO-d₆): δ 12.3, 24.1, 25.3, 27.4, 28.4, 37.3, 42.0, 57.8, 60.8, 69.7, 71.1, 104.1, 119.4, 121.5, 126.4, 127.3, 131.5, 137.7, 144.2, 147.9, 149.7, 156.0; HPLC-MS-ESI⁺ (*m/z*): [M + H]⁺ calculated for C₆₆H₇₉N₆O₆: 1051.60, found: 1051.8.

Hub⁴-cinchona

To a mixture of triazide (**10**, 110 mg, 0.45 mmol, 1.0 eq), cinchona derivative **9** (875 mg, 2.71 mmol, 6.0 eq) and DIPEA (1.66 mL, 9.49 mmol, 21.0 eq)—a suspension of CuI (51.7 mg, 0.27 mmol, 0.6 eq) in MeCN (3 mL)—were added. The mixture was stirred at 60 °C for 2 days. After complete consumption of the starting material (TLC, silica gel, MeOH/DCM/NH₄OH 1:5:0.01, or DCM/hexane 1:2), the solvent was evaporated under reduced pressure, and the crude product was purified by column chromatography (aluminum oxide, MeOH/DCM/NH₄OH 1:20:0.01–1:5:0.01 to yield **Hub⁴-cinchona** (306 mg, 56%) as a light-brown solid.

R_f: 0.49 (aluminum oxide, MeOH/DCM/NH₄OH 1:20:0.01); Mp. 179–180 °C; ¹H NMR (600 MHz, DMSO-d₆): δ 1.53 (m, 3H), 1.57 (m, 6H), 1.71 (m, 3H), 1.98 (m, 3H), 2.52 (m, 3H), 2.87 (m, 3H), 2.96 (m, 3H), 3.02 (m, 3H), 3.20 (m, 3H), 3.21 (m, 3H), 3.88 (s, 9H), 5.23 (m, 3H), 5.46 (s, 6H), 5.62 (d, *J* = 5.1 Hz, 3H), 7.08 (s, 3H), 7.38 (dd, *J* = 2.8; 9.2 Hz, 3H), 7.48 (d, *J* = 4.5 Hz, 3H), 7.51 (d, *J* = 4.5 Hz, 3H), 7.92 (d, *J* = 9.2 Hz, 3H), 7.93 (s, 3H), 8.86 (d, *J* = 4.5 Hz, 3H); ¹³C NMR (125 MHz, DMSO-d₆): δ 24.5, 27.5, 27.7, 32.8, 42.1, 52.4, 55.5, 55.6, 60.6, 71.1, 102.7, 119.4, 121.2, 122.2, 126.9, 127.4, 131.3, 137.6, 144.1, 147.7, 149.5; 150.7; 156.9; HPLC-MS-ESI⁺ (*m/z*): [M + H]⁺ calculated for C₆₉H₇₆N₁₅O₆: 1210.60, measured: 1210.40; HRMS-ESI⁺ (*m/z*): [M + H]⁺ calculated for C₆₉H₇₆N₁₅O₆: 1210.60975, found: 1210.61203.

General procedure for the indole hydroxyalkylation reaction: ethyl (S)-(+)-3,3,3-trifluoro-2-hydroxy-2-(1H-indol-3-yl)propanoate (13)

To a solution of indole (**11**, 36 mg, 0.31 mmol, 1.0 eq) in the given solvent (1 mL), hydroquinine (**1**, 5 mg, 0.015 mmol, 5 mol%) was added and the resulting reaction mixture was stirred for 1 h at 0 °C. Next, ethyl trifluoropyruvate (**12**, 27 μL, 0.31 mmol, 1.0 eq) was added to it, and stirred further at 0 °C. After the corresponding reaction time (see Tables 1–3) the volatile components were removed under reduced pressure. The crude product was purified by preparative thin-layer chromatography (R_f: 0.45, silica gel, DCM) to give product **13** as a solid.

R_f: 0.45 (silica gel, DCM); [α]_D²⁵: +9.1 (CHCl₃, *c* 1.00, 87% ee, *S* config.) (lit. [α]_D²⁵: +11.3, CHCl₃, *c* 1.01, 74% ee, *S* config. [57]); Colorless crystals. Mp. 71–72 °C (lit. Mp: 70.5–71.8 °C, [58]); MS-ESI⁻ (*m/z*): [M – H]⁻ 286; The yield was determined by ¹⁹F NMR. Enantiomeric excess was determined by reversed phase HPLC analysis using Phenomenex Lux Cellulose-1 (5 μm, 250 × 4.6 mm) column, eluent water (0.1% NH₄OAc)/MeCN = 40/60, 0.8 mL min⁻¹, UV detector 222 nm. Retention time for (*R*)-**13** and (*S*)-**13** are 6.5 min and 7.2 min, respectively. Spectroscopic data are fully consistent with those reported in the literature [58].

General procedure for the Michael addition reaction of pentane-2,4-dione (16):

To a solution of 1,3-dioxo compound **14** (78 μL, 0.77 mmol, 2.5 eq) and *trans*-β-nitrostyrene (**15**, 46 mg, 0.31 mmol, 1.0 eq) in the given solvent (1 mL), hydroquinine (**1**, 5 mg, 0.015 mmol, 5 mol%) was added. The resulting mixture was stirred at room temperature for 24 h. Then, the volatile components were removed under reduced pressure. The crude product was purified by thin-layer chromatography (hexane/EtOAc, 2:1) to give the Michael adduct as a solid.

(*S*)-(+)-3-(2-Nitro-1-phenylethyl)pentane-2,4-dione (**16**): R_f: 0.13 (silica gel, hexane/EtOAc, 4:1); [α]_D²⁵: +195.2 (CHCl₃, *c* 1.00, 99.1% ee, *S* config.) (lit. [α]_D²⁵: +196.7, CHCl₃, *c* 1.01, 88% ee, *S* config. [59]); White crystals. Mp. 125–128 °C (lit. Mp: 124–126 °C, [59]); MS-ESI⁺ (*m/z*): [M + NH₄]⁺ 267.1; Enantiomeric excess was determined by normal phase HPLC analysis using Phenomenex Lux Cellulose-1 column (5 μm, 250 × 4.6 mm), eluent hexane/ethanol = 85/15, isocratic mode; 0.8 mL min⁻¹; temperature 20 °C, UV detector 254 nm. Retention time for (*S*)-**16**: 16.1 min, for (*R*)-**16**: 17.6 min. Spectroscopic data are fully consistent with those reported in the literature [59].

General procedure for the Michael addition reaction of 1,3-diphenylpropan-1,3-dione (**18**):

To a solution of 1,3-dioxo compound **17** (107 mg, 0.48 mmol, 1.0 eq) and *trans*- β -nitrostyrene (**15**, 213 mg, 1.43 mmol, 3.0 eq) in the given solvent (2 mL), hydroquinine (**1**, 5 mg, 0.015 mmol, 5 mol%) was added. The resulting mixture was stirred at room temperature for 24 h. Then, the volatile components were removed under reduced pressure. The crude product was purified by thin-layer chromatography (hexane/EtOAc, 4:1) to give the Michael adduct as a solid.

(*S*)-(+)-2-(2-Nitro-1-phenylethyl)-1,3-diphenylpropane-1,3-dione (**18**): R_f : 0.35 (silica gel, hexane/EtOAc, 4:1); $[\alpha]_D^{25}$: +22.1 (DCM, c 1.0, 99.3% ee, *S* config.) (lit. $[\alpha]_D^{25}$: +21.3, DCM, c 1.0, 98% ee, *S* config. [60]); White crystals. Mp. 136.2 °C (lit. Mp: 135.6 °C [61]); MS-ESI+ (m/z): $[M + H]^+$ 391.2. When **Hub**¹⁻⁴-**cinchonas** were used as catalysts, enantiomeric excess was determined by reversed phase HPLC analysis using Phenomenex Lux Cellulose-1 column (5 μ m, 250 \times 4.6 mm), eluent water (0.1% NH₄OAc)/MeCN = 30/70, isocratic mode; 0.8 mL·min⁻¹, temperature 20 °C, UV detector 222 nm. Retention time for (*S*)-**18**: 7.6 min, for (*R*)-**18**: 8.9 min. When hydroquinine (**1**) was used as a catalyst, enantiomeric excess value was determined by normal phase HPLC analysis with Kromasil® 5-Amycoat column (250 \times 4.6 mm ID, 5 μ m) using hexane/ethanol (85:15) eluent. Retention time for (*R*)-**18**: 19.2 min, for (*S*)-**18**: 26.1 min. Spectroscopic data are fully consistent with those reported in the literature [61].

3.3. Nanofiltration

Membrane separation was carried out in a crossflow nanofiltration rig with 53 cm² effective area (*A*), as described in the literature [62]. PolarClean, as a green solvent [63], was used for the filtration, and the applied pressure was 10 bar. Two independent measurements were carried out, and the presented results are mean values. Equations (1) and (2) were used to calculate the rejection and permeance after 24 h recirculation in the rig, respectively.

$$\text{Rejection [\%]} = \left(1 - \frac{C_p}{C_f}\right) \times 100\% \quad (1)$$

$$\text{Flux [L m}^{-2} \text{ h}^{-1}] = \frac{V}{A \cdot t} \quad (2)$$

where C_p and C_f are the permeate and feed concentrations of the solutes, respectively; V is the permeate volume, while t is the time of solvent permeation through the membrane with certain membrane area (*A*).

4. Conclusions

Four structurally different C₃-symmetric cinchona organocatalysts were prepared, in which the catalytic units are covalently anchored to a trifunctional central core (hub). Depending on the immobilization site, we obtained compounds either containing or lacking mono H-bond donor groups on the cinchona skeleton.

The catalytic activities of these size-enlarged molecules were tested in the hydroxyalkylation of indole and Michael addition reaction. While the parent hydroquinine was found to be an efficient catalyst for the Friedel–Crafts reaction of indole (up to 73% ee), the hub-cinchona catalysts showed significantly lower enantioselectivities, regardless of the solvent applied. The structure–selectivity correlations revealed that catalysts with more rigid and extensive spacers performed better, suggesting a disadvantageous interaction of the individual cinchona units. On the contrary, in the Michael addition reaction, the hub-cinchona catalyst showed increased selectivity compared to hydroquinine, which indicates the positive effect of the C₃-symmetric structure. Furthermore, **Hub**³-**cinchona** was also shown to provide enantioselectivities up to 96% ee, in the case of a bulkier substrate. Finally, membrane recovery of the size-enlarged organocatalysts using the PolarClean alternative solvent was found to be straightforward thanks to their ~four-fold increase in size compared to hydroquinine.

Supplementary Materials: The following are available online at <https://www.mdpi.com/2073-8994/13/3/521/s1>.

Author Contributions: Methodology, P.K. (Péter Kisszékelyi), Z.F., S.N. and J.K.; synthesis of compounds, P.K. (Petra Kozma), Z.F., S.N. and P.K. (Péter Kisszékelyi); determination of ee values by chiral HPLC measurements, P.B. and B.M.; performed NMR experiments, data analysis, Z.G.; performed MS measurements, data analysis, M.D. and B.M.; writing—original draft preparation, P.K. (Péter Kisszékelyi); writing—review and editing, J.K., Z.F., S.N., P.K. (Péter Kisszékelyi), P.B. and P.H.; project administration, J.K.; funding acquisition, P.H. and J.K.; resources, P.H. and J.K.; supervision, J.K. All authors have read and agreed to the published version of the manuscript.

Funding: This research was funded by the New National Excellence Program of the Ministry of Human Capacities, grant numbers ÚNKP-20-4-I-BME-320 (Péter Kisszékelyi), ÚNKP-20-3-II-BME-325 (S.N.) and ÚNKP-20-5-BME-322 (J.K.), and the János Bolyai Research Scholarship of the Hungarian Academy of Science (J.K.). It was also supported by the National Research, Development, and Innovation Office (grant number K128473), the Servier–Beregi PhD Research Fellowship (S.N.), and the Gedeon Richter’s Talentum Foundation (Péter Kisszékelyi and Z.F.). This work was also funded by the Cooperative Doctoral Program Doctoral Student Scholarship (KDP-2020-1007075) of the Ministry of Innovation and Technology (Z.G.).

Institutional Review Board Statement: Not applicable.

Informed Consent Statement: Not applicable.

Data Availability Statement: All data created and analyzed in this study can be found within the article or supplementary material. Therefore we would not select any Data Availability Statement from MDPI Research Data Policies.

Acknowledgments: The authors are grateful to András Dancsó from Egis Pharmaceuticals Plc., Directorate of Drug Substance Development, for his assistance with the NMR measurements.

Conflicts of Interest: The authors declare no conflict of interest.

References

1. Kamer, P.; Vogt, D.; Thybaut, J.W. (Eds.) *Contemporary Catalysis: Science, Technology, and Applications*, Gld. ed.; The Royal Society of Chemistry: London, UK, 2017.
2. Jacobsen, E.N.; Pfaltz, A.; Yamamoto, H. *Comprehensive Asymmetric Catalysis I–III (Comprehensive Overviews in Chemistry)*, 1st ed.; Springer: Berlin/Heidelberg, Germany, 1999.
3. Moberg, C. C₃ Symmetry in Asymmetric Catalysis and Chiral Recognition. *Angew. Chem. Int. Ed.* **1998**, *37*, 248–268. [[CrossRef](#)]
4. Moberg, C. The Role of Symmetry in Asymmetric Catalysis. *Isr. J. Chem.* **2012**, *52*, 653–662. [[CrossRef](#)]
5. Gade, L.H.; Bellemin-Lapponnaz, S. Exploiting Threefold Symmetry in Asymmetric Catalysis: The Case of Tris(oxazoliny)ethanes (“Trisox”). *Chem. A Eur. J.* **2008**, *14*, 4142–4152. [[CrossRef](#)]
6. Gibson, S.E.; Castaldi, M.P. Applications of chiral C₃-symmetric molecules. *Chem. Commun.* **2006**, *37*, 3045–3062. [[CrossRef](#)]
7. Rodríguez, L.-I.; Roth, T.; Fillol, J.L.; Wade, H.; Gade, L.H. The More Gold-The More Enantioselective: Cyclohydroaminations of γ -Allenyl Sulfonamides with Mono-, Bis-, and Trisphospholane Gold(I) Catalysts. *Chem. A Eur. J.* **2012**, *18*, 3721–3728. [[CrossRef](#)]
8. Yamanaka, M.; Nakagawa, T.; Aoyama, R.; Nakamura, T. Synthesis and estimation of gelation ability of C₃-symmetry tris-urea compounds. *Tetrahedron* **2008**, *64*, 11558–11567. [[CrossRef](#)]
9. Crişan, C.V.; Soran, A.; Bende, A.; Hädade, N.D.; Terec, A.; Grosu, I. Synthesis, Structure and Supramolecular Properties of a Novel C₃ Cryptand with Pyridine Units in the Bridges. *Molecules* **2020**, *25*, 3789. [[CrossRef](#)] [[PubMed](#)]
10. Yu, M.-H.; Liu, X.-T.; Space, B.; Chang, Z.; Bu, X.-H. Metal-organic materials with triazine-based ligands: From structures to properties and applications. *Co-ord. Chem. Rev.* **2021**, *427*, 213518. [[CrossRef](#)]
11. García, A.; Insuasty, B.; Herranz, M.A.; Martínez-Álvarez, R.; Martín, N. New Building Block for C₃ Symmetry Molecules: Synthesis of Triazine-Based Redox Active Chromophores. *Org. Lett.* **2009**, *11*, 5398–5401. [[CrossRef](#)]
12. Burns, B.; King, N.P.; Tye, H.; Studley, J.R.; Gamble, M.; Wills, M. Chiral phosphinamides: New catalysts for the asymmetric reduction of ketones by borane. *J. Chem. Soc. Perkin Trans.* **1998**, *1*, 1027–1038. [[CrossRef](#)]
13. Du, D.-M.; Fang, T.; Xu, J.; Zhang, S.-W. Structurally Well-Defined, Recoverable C₃-Symmetric Tris(β -hydroxy phosphoramidate)-Catalyzed Enantioselective Borane Reduction of Ketones. *Org. Lett.* **2006**, *8*, 1327–1330. [[CrossRef](#)] [[PubMed](#)]
14. Wang, Y.; Wang, L.; Pan, Y.; Han, J.; Wu, H.; Teng, M.; Li, Z. Novel Tripod 1-Prolineamide Catalysts Based on Tribenzyl- and Triphenyl-phosphine Oxide for the Direct Aldol Reaction. *Synlett* **2009**, *2009*, 933–936. [[CrossRef](#)]
15. Moorthy, J.N.; Saha, S. C₃-Symmetric Proline-Functionalized Organocatalysts: Enantioselective Michael Addition Reactions. *Eur. J. Org. Chem.* **2010**, *2010*, 6359–6365. [[CrossRef](#)]

16. Murai, K.; Fukushima, S.; Hayashi, S.; Takahara, Y.; Fujioka, H. C₃-Symmetric Chiral Trisimidazoline: Design and Application to Organocatalyst. *Org. Lett.* **2010**, *12*, 964–966. [[CrossRef](#)]
17. Murai, K.; Fukushima, S.; Nakamura, A.; Shimura, M.; Fujioka, H. C₃-Symmetric chiral trisimidazoline: The role of a third imidazoline and its application to the nitro Michael reaction and the α -amination of β -ketoesters. *Tetrahedron* **2011**, *67*, 4862–4868. [[CrossRef](#)]
18. Murai, K.; Nakamura, A.; Matsushita, T.; Shimura, M.; Fujioka, H. C₃-Symmetric Trisimidazoline-Catalyzed Enantioselective Bromolactonization of Internal Alkenoic Acids. *Chem. A Eur. J.* **2012**, *18*, 8448–8453. [[CrossRef](#)]
19. Takizawa, S.; Sako, M.; Abozeid, M.A.; Kishi, K.; Wathsala, H.D.P.; Hirata, S.; Murai, K.; Fujioka, H.; Sasai, H. Enantio- and Diastereoselective Betti/aza-Michael Sequence: Single Operated Preparation of Chiral 1,3-Disubstituted Isoindolines. *Org. Lett.* **2017**, *19*, 5426–5429. [[CrossRef](#)]
20. Boratyński, P.J. Dimeric Cinchona alkaloids. *Mol. Divers.* **2015**, *19*, 385–422. [[CrossRef](#)]
21. Park, H.-G.; Jeong, B.-S.; Yoo, M.-S.; Park, M.-K.; Huh, H.; Jew, S.-S. Trimeric Cinchona alkaloid phase-transfer catalyst: $\alpha, \alpha', \alpha''$ -tris[O(9)-allyl]cinchonidinium]mesitylene tribromide. *Tetrahedron Lett.* **2001**, *42*, 4645–4648. [[CrossRef](#)]
22. Siva, A.; Murugan, E. A New Trimeric Cinchona Alkaloid as a Chiral Phase-Transfer Catalyst for the Synthesis of Asymmetric α -Amino Acids. *Synthesis* **2005**, *2005*, 2927–2933. [[CrossRef](#)]
23. Siva, A.; Murugan, E. New trimeric Cinchona alkaloid-based quaternary ammonium salts as efficient chiral phase transfer catalysts for enantioselective synthesis of α -amino acids. *J. Mol. Catal. A Chem.* **2006**, *248*, 1–9. [[CrossRef](#)]
24. Siva, A.; Jayaraman, S.; Kumaraguru, D.; Arockiam, J.B.; Paulpandian, S.; Rajendiran, B. Highly Enantioselective Asymmetric Michael Addition Reactions with New Chiral Multisite Phase-Transfer Catalysts. *Synlett* **2014**, *25*, 1685–1691. [[CrossRef](#)]
25. Beneto, A.J.; Sivamani, J.; AshokKumar, V.; Duraimurugan, K.; Balasaravanan, R.; Siva, A. Highly enantioselective Michael addition reactions with new trimeric chiral phase transfer catalysts. *New J. Chem.* **2015**, *39*, 3098–3104. [[CrossRef](#)]
26. Károlyi, B.I.; Bősze, S.; Orbán, E.; Sohár, P.; Drahos, L.; Gál, E.; Csámpai, A. Acylated mono-, bis- and tris- Cinchona-Based Amines Containing Ferrocene or Organic Residues: Synthesis, Structure and in Vitro Antitumor Activity on Selected Human Cancer Cell Lines. *Molecules* **2012**, *17*, 2316–2329. [[CrossRef](#)]
27. Min, C.; Han, X.; Liao, Z.; Wu, X.; Zhou, H.-B.; Dong, C. C₃-Symmetrical Cinchonine-Squaramide as New Highly Efficient, and Recyclable Organocatalyst for Enantioselective Michael Addition. *Adv. Synth. Catal.* **2011**, *353*, 2715–2720. [[CrossRef](#)]
28. Han, X.; Liu, B.; Zhou, H.-B.; Dong, C. Enhanced efficiency of recyclable C₃-symmetric cinchonine-squaramides in the asymmetric Friedel–Crafts reaction of indoles with alkyl trifluoropyruvate. *Tetrahedron Asymmetry* **2012**, *23*, 1332–1337. [[CrossRef](#)]
29. Han, X.; Dong, C.; Zhou, H.-B. C₃-Symmetric Cinchonine-Squaramide-Catalyzed Asymmetric Chlorolactonization of Styrene-Type Carboxylic Acids with 1,3-Dichloro-5,5-dimethylhydantoin: An Efficient Method to Chiral Isochroman-1-ones. *Adv. Synth. Catal.* **2014**, *356*, 1275–1280. [[CrossRef](#)]
30. Lv, W.; Guo, C.; Dong, Z.; Tang, S.; Liu, B.; Dong, C. C₃-Symmetric cinchonine-squaramide as a recyclable efficient organocatalyst for tandem Michael addition–cyclisation of malononitrile and nitrovinylphenols. *Tetrahedron Asymmetry* **2016**, *27*, 670–674. [[CrossRef](#)]
31. Le Phuong, H.A.; Blanford, C.F.; Szekely, G. Reporting the unreported: The reliability and comparability of the literature on organic solvent nanofiltration. *Green Chem.* **2020**, *22*, 3397–3409. [[CrossRef](#)]
32. Hu, J.; Kim, C.; Halasz, P.; Kim, J.F.; Kim, J.; Szekely, G. Artificial intelligence for performance prediction of organic solvent nanofiltration membranes. *J. Membr. Sci.* **2021**, *619*, 118513. [[CrossRef](#)]
33. Le Phuong, H.A.; Cseri, L.; Whitehead, G.F.S.; Garforth, A.; Budd, P.; Szekely, G. Environmentally benign and diastereoselective synthesis of 2,4,5-trisubstituted-2-imidazolines. *RSC Adv.* **2017**, *7*, 53278–53289. [[CrossRef](#)]
34. Dong, R.; Liu, R.; Gaffney, P.R.J.; Schaepertoens, M.; Marchetti, P.; Williams, C.M.; Chen, R.; Livingston, A.G. Sequence-defined multifunctional polyethers via liquid-phase synthesis with molecular sieving. *Nat. Chem.* **2019**, *11*, 136–145. [[CrossRef](#)] [[PubMed](#)]
35. Székely, G.; Schaepertoens, M.; Gaffney, P.R.J.; Livingston, A.G. Beyond PEG2000: Synthesis and Functionalisation of Monodisperse PEGylated Homostars and Clickable Bivalent Polyethyleneglycols. *Chem. A Eur. J.* **2014**, *20*, 10038–10051. [[CrossRef](#)] [[PubMed](#)]
36. Razali, M.; Didaskalou, C.; Kim, J.F.; Babaei, M.; Drioli, E.; Lee, Y.M.; Szekely, G. Exploring and Exploiting the Effect of Solvent Treatment in Membrane Separations. *ACS Appl. Mater. Interfaces* **2017**, *9*, 11279–11289. [[CrossRef](#)]
37. Voros, V.; Drioli, E.; Fonte, C.; Szekely, G. Process Intensification via Continuous and Simultaneous Isolation of Antioxidants: An Upcycling Approach for Olive Leaf Waste. *ACS Sustain. Chem. Eng.* **2019**, *7*, 18444–18452. [[CrossRef](#)]
38. Alammari, A.; Park, S.-H.; Williams, C.J.; Derby, B.; Szekely, G. Oil-in-water separation with graphene-based nanocomposite membranes for produced water treatment. *J. Membr. Sci.* **2020**, *603*, 118007. [[CrossRef](#)]
39. Keraani, A.; Nasser, G.; Shahane, S.; Renouard, T.; Bruneau, C.; Rabiller-Baudry, M.; Fischmeister, C. Syntheses and characterization of molecular weight enlarged olefin metathesis pre-catalysts. *Comptes Rendus Chim.* **2017**, *20*, 717–723. [[CrossRef](#)]
40. Kisszékelyi, P.; Nagy, S.; Fehér, Z.; Huszthy, P.; Kupai, J. Membrane-Supported Recovery of Homogeneous Organocatalysts: A Review. *Chemistry* **2020**, *2*, 742–758. [[CrossRef](#)]
41. Siew, W.E.; Ates, C.; Merschaert, A.; Livingston, A.G. Efficient and productive asymmetric Michael addition: Development of a highly enantioselective quinidine-based organocatalyst for homogeneous recycling via nanofiltration. *Green Chem.* **2013**, *15*, 663–674. [[CrossRef](#)]
42. Shao, Z.; Zhang, H. Combining transition metal catalysis and organocatalysis: A broad new concept for catalysis. *Chem. Soc. Rev.* **2009**, *38*, 2745–2755. [[CrossRef](#)]
43. Zhong, C.; Shi, X. When Organocatalysis Meets Transition-Metal Catalysis. *Eur. J. Org. Chem.* **2010**, *2010*, 2999–3025. [[CrossRef](#)]

44. Didaskalou, C.; Kupai, J.; Cseri, L.; Barabas, J.; Vass, E.; Holtzl, T.; Szekely, G. Membrane-Grafted Asymmetric Organocatalyst for an Integrated Synthesis–Separation Platform. *ACS Catal.* **2018**, *8*, 7430–7438. [[CrossRef](#)]
45. Kisszekelyi, P.; Alammari, A.; Kupai, J.; Huszthy, P.; Barabas, J.; Holtzl, T.; Szente, L.; Bawn, C.; Adams, R.; Szekely, G. Asymmetric synthesis with cinchona-decorated cyclodextrin in a continuous-flow membrane reactor. *J. Catal.* **2019**, *371*, 255–261. [[CrossRef](#)]
46. Schaepertoens, M.; Didaskalou, C.; Kim, J.F.; Livingston, A.G.; Szekely, G. Solvent recycle with imperfect membranes: A semi-continuous workaround for diafiltration. *J. Membr. Sci.* **2016**, *514*, 646–658. [[CrossRef](#)]
47. Zhao, D.; Kim, J.F.; Ignacz, G.; Pogany, P.; Lee, Y.M.; Szekely, G. Bio-Inspired Robust Membranes Nanoengineered from Interpenetrating Polymer Networks of Polybenzimidazole/Polydopamine. *ACS Nano* **2019**, *13*, 125–133. [[CrossRef](#)]
48. Ignacz, G.; Fei, F.; Szekely, G. Ion-Stabilized Membranes for Demanding Environments Fabricated from Polybenzimidazole and Its Blends with Polymers of Intrinsic Microporosity. *ACS Appl. Nano Mater.* **2018**, *1*, 6349–6356. [[CrossRef](#)]
49. Cassani, C.; Martín-Rapún, R.; Arceo, E.; Bravo, F.; Melchiorre, P. Synthesis of 9-amino(9-deoxy)epi cinchona alkaloids, general chiral organocatalysts for the stereoselective functionalization of carbonyl compounds. *Nat. Protoc.* **2013**, *8*, 325–344. [[CrossRef](#)] [[PubMed](#)]
50. Skarżewski, J.; Zielińska-Błajet, M.; Kucharska, M. Simple Enantiospecific Synthesis of Sulfides of Cinchona Alkaloids. *Synthesis* **2006**, *2006*, 1176–1182. [[CrossRef](#)]
51. Yaegashi, K.; Mikami, M. Preparation of 9-azido Cinchona Alkaloids, Their 9-amino Derivatives, and Their 9-(substituted thioureido) Derivatives. JP Patent 2010024173 (20100204), 4 February 2010.
52. Heidelberger, M.; Jacobs, W.A. Syntheses in the cinchona series. I. The simpler cinchona alkaloids and their dihydro derivatives. *J. Am. Chem. Soc.* **1919**, *41*, 817–833. [[CrossRef](#)]
53. Brandes, S.; Niess, B.; Bella, M.; Prieto, A.; Overgaard, J.; Jørgensen, K.A. Non-Biaryl Atropisomers in Organocatalysis. *Chem. A Eur. J.* **2006**, *12*, 6039–6052. [[CrossRef](#)]
54. Braje, W.M.; Frackenhohl, J.; Schrage, O.; Wartchow, R.; Beil, W.; Hoffmann, H.M.R. Synthesis of 10,11-DidehydroCinchona Alkaloids and Key Derivatives. *Helvetica Chim. Acta* **2000**, *83*, 777–792. [[CrossRef](#)]
55. Song, Y.; Kohlmeier, E.K.; Meade, T.J. Synthesis of Multimeric MR Contrast Agents for Cellular Imaging. *J. Am. Chem. Soc.* **2008**, *130*, 6662–6663. [[CrossRef](#)] [[PubMed](#)]
56. Gilbert, E.E.; Voreck, W.E. Evaluation of a new organic azide: Hexakis(azidomethyl)benzene (HAB). *Propellants Explos. Pyrotech.* **1989**, *14*, 19–23. [[CrossRef](#)]
57. Lyle, M.P.A.; Draper, N.D.; Wilson, P.D. Enantioselective Friedel–Crafts Alkylation Reactions Catalyzed by a Chiral Nonracemic C₂-Symmetric 2,2′-Bipyridyl Copper(II) Complex. *Org. Lett.* **2005**, *7*, 901–904. [[CrossRef](#)]
58. Török, B.; Abid, M.; London, G.; Esquibel, J.; Török, M.; Mhadgut, S.C.; Yan, P.; Prakash, G.K.S. Highly Enantioselective Organocatalytic Hydroxyalkylation of Indoles with Ethyl Trifluoropyruvate. *Angew. Chem. Int. Ed.* **2005**, *44*, 3086–3089. [[CrossRef](#)]
59. Evans, D.A.; Mito, A.S.; Seidel, D. Scope and Mechanism of Enantioselective Michael Additions of 1,3-Dicarbonyl Compounds to Nitroalkenes Catalyzed by Nickel(II)–Diamine Complexes. *J. Am. Chem. Soc.* **2007**, *129*, 11583–11592. [[CrossRef](#)]
60. Tan, B.; Zhang, X.; Chua, P.J.; Zhong, G. Recyclable organocatalysis: Highly enantioselective Michael addition of 1,3-diaryl-1,3-propanedione to nitroolefins. *Chem. Commun.* **2009**, 779–781. [[CrossRef](#)]
61. Gonczi, K.; Kudar, V.; Jaszay, Z.; Bombicz, P.; Faigl, F.; Madarász, J. Solid state structural relation and binary melting phase diagram of (S-) and racemic 2-(2-nitro-1-phenylethyl)-1,3-diphenyl-propane-1,3-dione. *Thermochim. Acta* **2014**, *580*, 46–52. [[CrossRef](#)]
62. Fei, F.; Le Phuong, H.A.; Blanford, C.F.; Szekely, G. Tailoring the Performance of Organic Solvent Nanofiltration Membranes with Biophenol Coatings. *ACS Appl. Polym. Mater.* **2019**, *1*, 452–460. [[CrossRef](#)]
63. Cseri, L.; Szekely, G. Towards cleaner PolarClean: Efficient synthesis and extended applications of the polar aprotic solvent methyl 5-(dimethylamino)-2-methyl-5-oxopentanoate. *Green Chem.* **2019**, *21*, 4178–4188. [[CrossRef](#)]